Supporting Information

# A Core/Shell Nanogenerator Achieving pH-Responsive Nitric Oxide Release for Treatment of Infected Diabetic Wounds

*Yaming Zhou*[a], *Yanjie Jiang*[a], *Jingfeng Cai*[a], *Jiaping Wang*[a], *Sen Zeng*[a], *Shuo Li*[b], *Miao Wang*[a], *Xi Zhou*[a], *Xiumin Wang*[c], *Xueqin Zhao*[b, *], *Lei Ren*[a, d, *]

[a] The Higher Educational Key Laboratory for Biomedical Engineering of Fujian Province, Research Center of Biomedical Engineering of Xiamen, Department of Biomaterials, College of Materials, Xiamen University, Xiamen 361005, People's Republic of China.

[b] College of Life Sciences and Medicine, Zhejiang Sci-Tech University, Hangzhou 310018, People's Republic of China.

[c] School of Pharmaceutical Sciences, Xiamen University, Xiamen, 361102, People's Republic of China.

[d] State Key Laboratory of Physical Chemistry of Solid Surfaces, College of Chemistry and Chemical Engineering, Xiamen University, Xiamen 361005, People's Republic of China.

***Lei Ren** E-mail: *renlei@xmu.edu.cn*

*** Xueqin Zhao** E-mail: *zhaoxueqin@zstu.edu.cn*

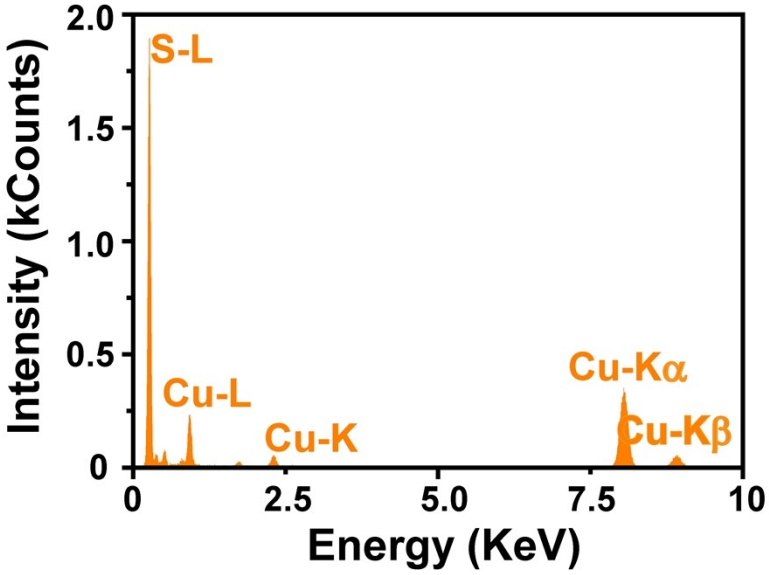


**Fig. S1.** Chemical elements present on sample of the CuS nanospheres.

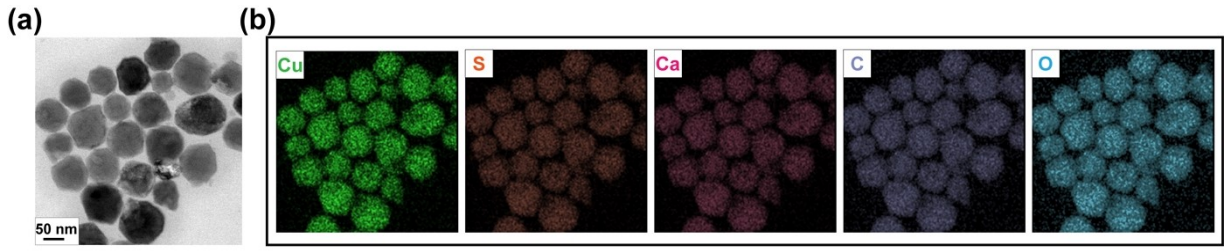


**Fig. S2.** (a) The selected TEM image and (b) element mappings of the CuS@$CaCO_3$ nanostructures. (bar scale: 50 nm)

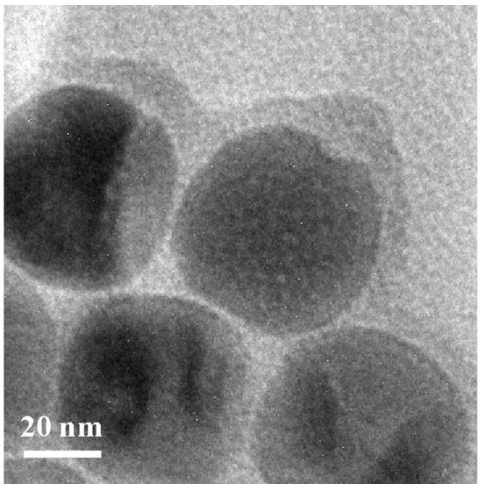


**Fig. S3.** TEM image of ISDN-ligands coated on the core/shell nanoparticles.

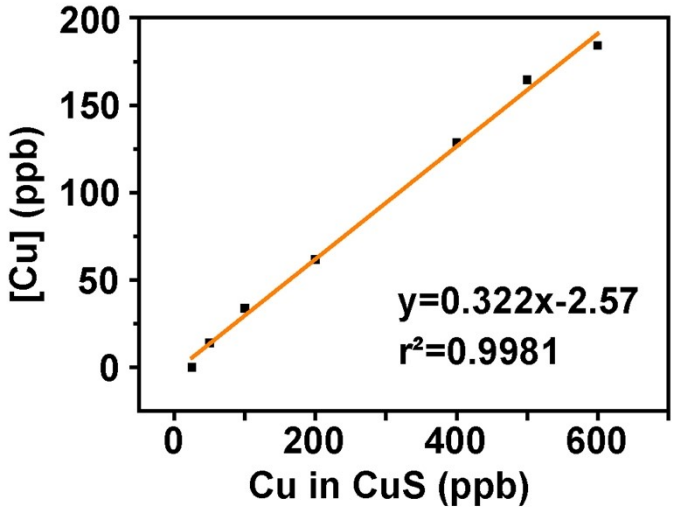


**Fig. S4.** ICP analysis of Cu in the CuS@$CaCO_3$.

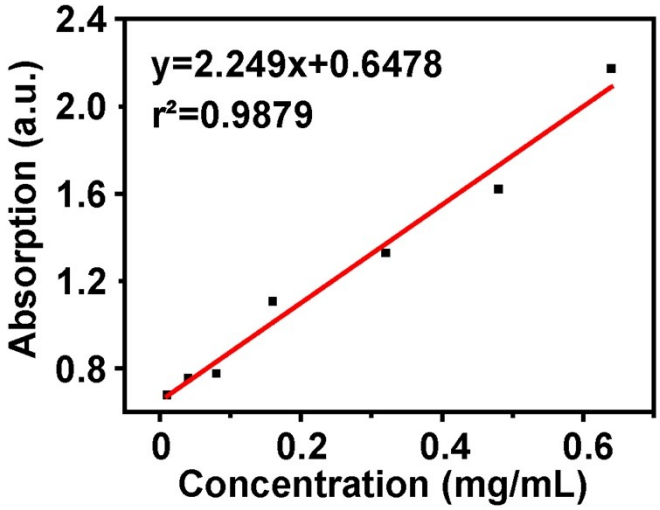


**Fig. S5.** Determination of ISDN content by UV absorption.

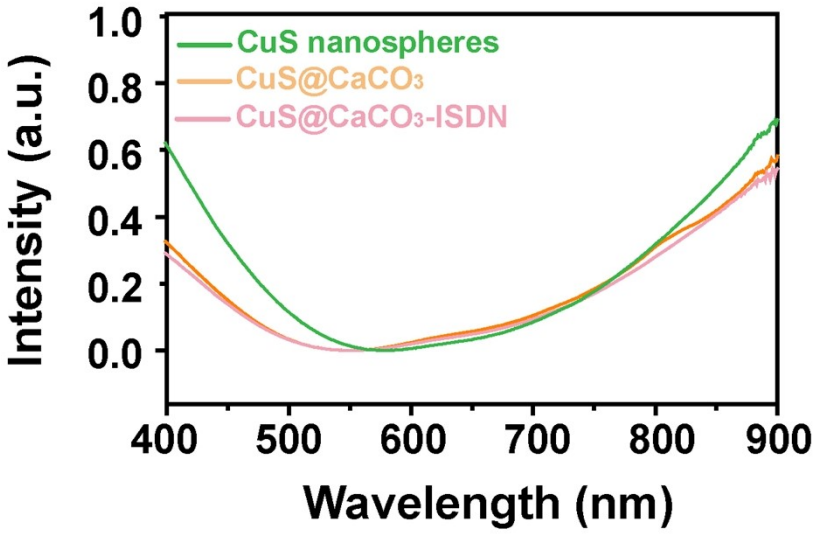


**Fig. S6.** UV–Vis spectra of different nanostructures (Concentrations of CuS in CuS@$CaCO_3$, CuS and CuS@$CaCO_3$-ISDN: 0.4 mg/mL).

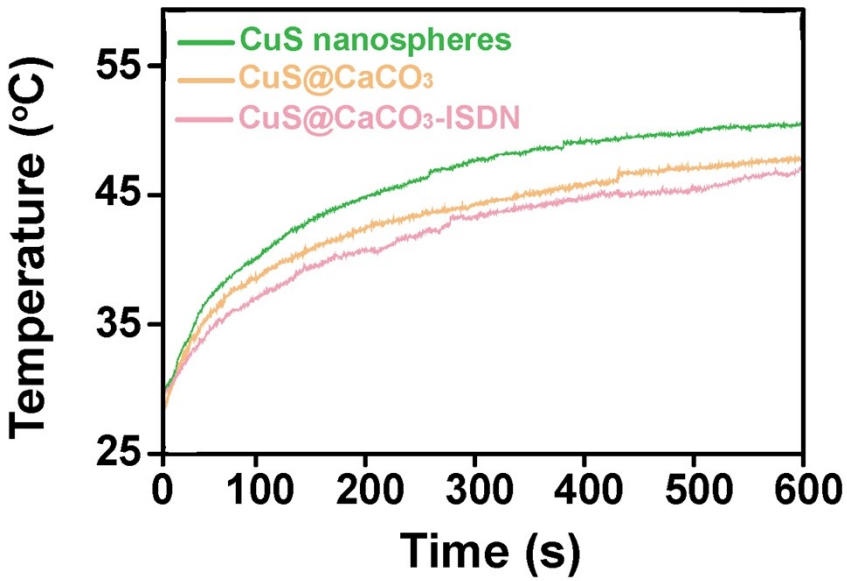


**Fig. S7.** Photothermal heating curves of different nanostructures (Concentrations of CuS in $CuS@CaCO_3$, CuS and $CuS@CaCO_3$-ISDN: 0.4 mg/mL, NIR: 808 nm, 1.0 W/cm$^2$).

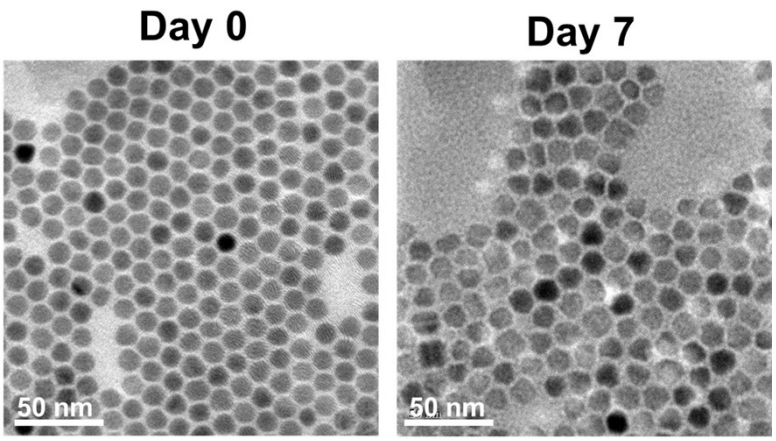


**Fig. S8.** The TEM images of CuS nanoparticles on day 0 and day 7.

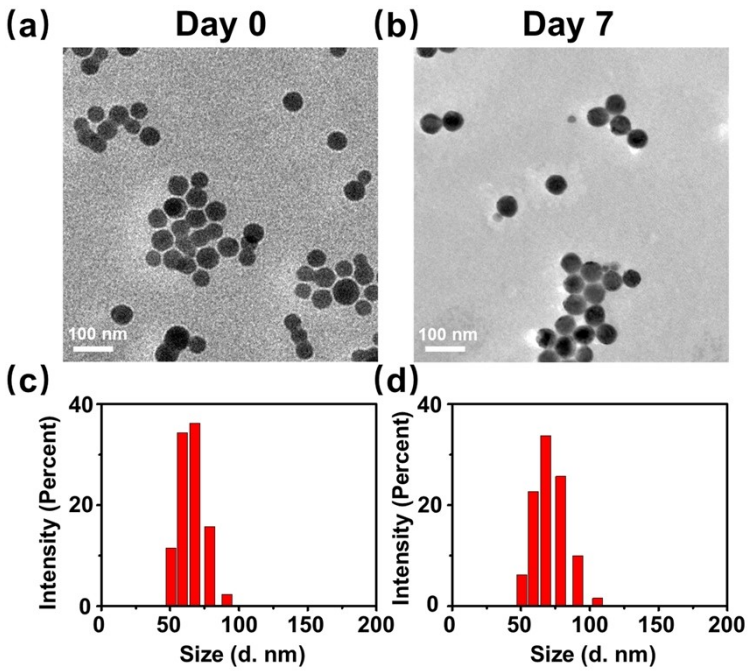


**Fig. S9.** TEM images (a-b) and DLS assay (c-d) of CuS@$CaCO_3$-ISDN on day 0 and day 7.

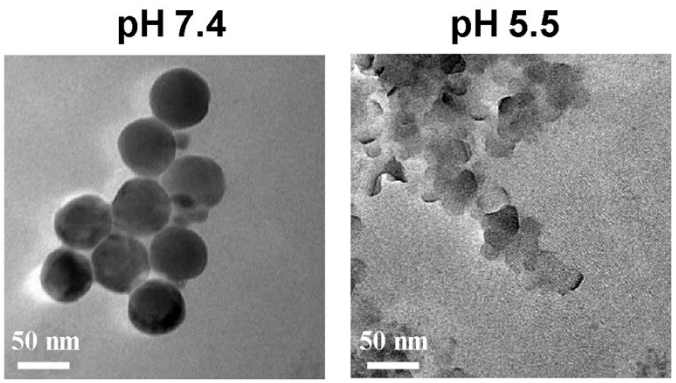


**Fig. S10.** Representative TEM images of CuS@$CaCO_3$-ISDN after being immersed in buffers with different pH values (7.4 and 5.5) for 2h.

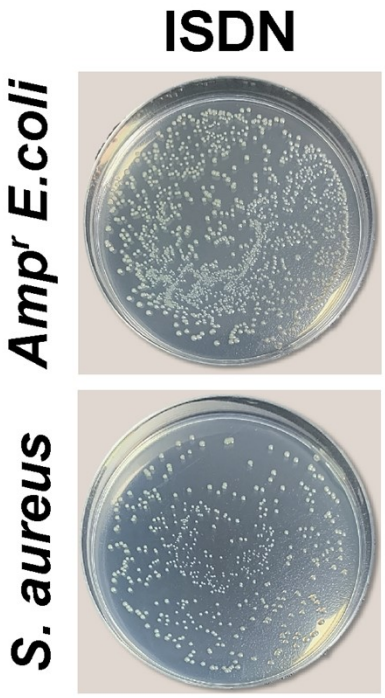


**Fig. S11.** The antibacterial performance of ISDN (0.1 mg/mL).

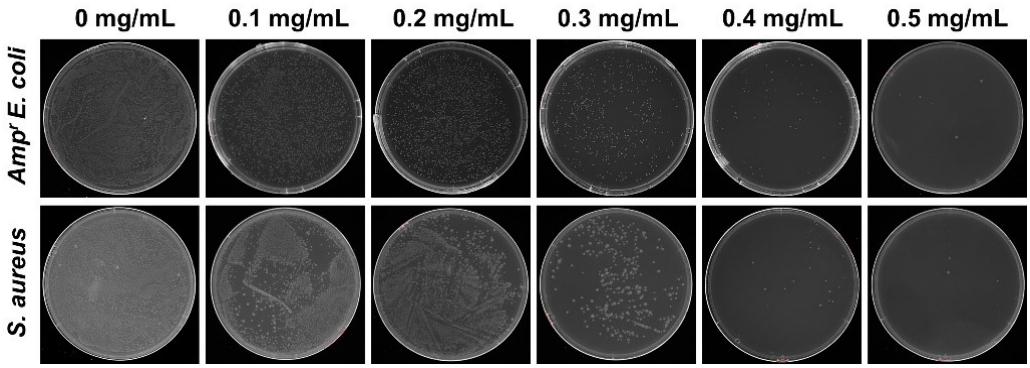


**Fig. S12.** The antibacterial performance of NIR-assisted CuS@$CaCO_3$-ISDN at different concentrations (0-0.5 mg/mL). (NIR irradiation: 808 nm, 1.0 W/$cm^2$, 10 min)

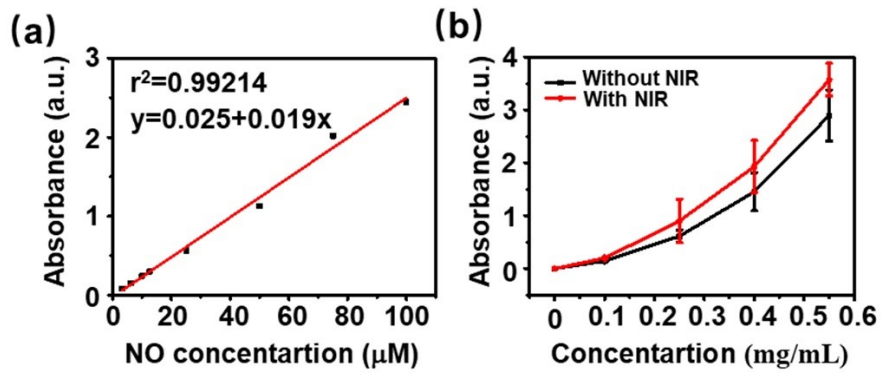


**Fig. S13.** (a) Standard curve of NO generation. (b) NO release from different concentrations of CuS@$CaCO_3$-ISDN with or without NIR irradiation (808 nm, 1.0 W/$cm^2$, 10 min).

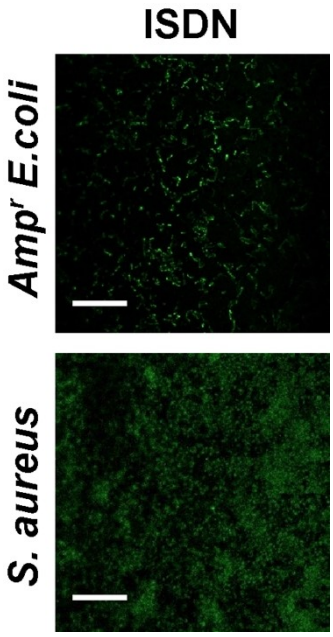


**Fig. S14.** Nitric oxide content of bacteria after ISDN treatment. (ISDN: 0.1 mg/mL)

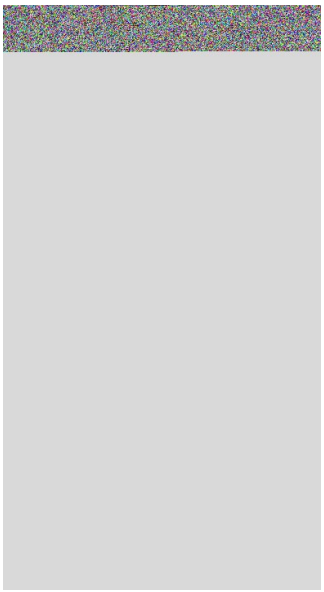

**Fig. S15.** ROS content of bacteria after ISDN treatment. (ISDN: 0.1 mg/mL)

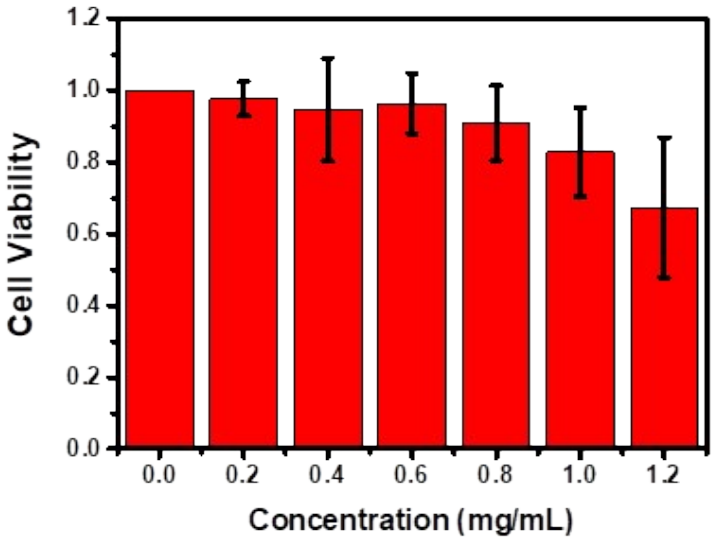


**Fig. S16.** Cell viability of HUVEC cells incubated with different concentrations of CuS@$CaCO_3$-ISDN.

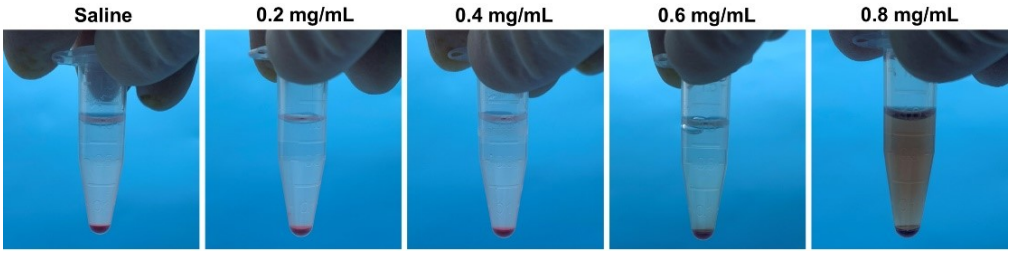


**Fig. S17.** Hemolysis assay of core/shell nanogenerator at different concentrations.

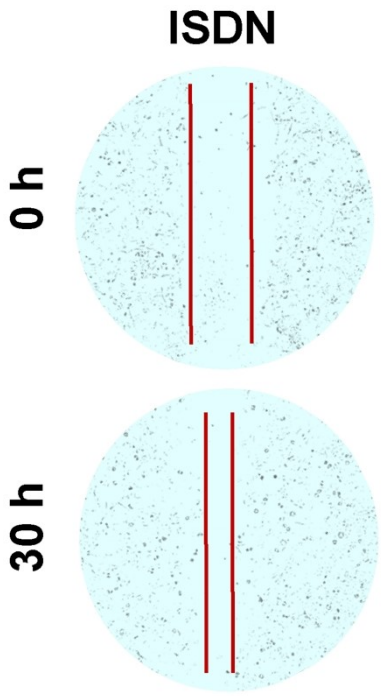


**Fig. S18.** Images of the migration assay after ISDN treatment. (ISDN: 0.1 mg/mL)